Sains Malaysiana 54(11)(2025): 2733-2744
http://doi.org/10.17576/jsm-2025-5411-13

Direct Oxidation of Various Oil Palm Components using CeO Catalyst for Vanillin Production

(Pengoksidaan Langsung Pelbagai Komponen Kelapa Sawit menggunakan Pemangkin CeO untuk Pengeluaran Vanilin)

ANITA RAMLI[1,2,*], NUR AKILA SYAKIDA IDAYU KHAIRUL ANUAR[1,2], FARINAA MD JAMIL[1,2], NAJMAN NAQIB KAMARUZAMAN[2], NURAZIEDA DAYANA ROZI[2], CHAM HUI JING[2], FARAH ANIS SYAFIQAH MD FARIZAL[2] & NUR MASITAH LAILY ZAMRI[2]

[1]HICoE Centre of Biofuel and Biochemical Research, Universiti Teknologi PETRONAS, 32610 Seri Iskandar, Perak, Malaysia
[2]Department of Applied Science, Universiti Tekknologi PETRONAS, 32610 Seri Iskandar, Perak, Malaysia

Received: 28 April 2025/Accepted: 30 September 2025

ABSTRACT

Vanillin has a significant market demand as it is consumed as raw materials in many daily products such as fragrances and pharmaceuticals. The supply chain is dominated by synthetic vanillin due to its preferred pathway and cost-effective manufacturing. The different palm oil biomass feedstocks, including fronds, trunks, empty fruit bunches, kernel shells, and mesocarp fibers, were evaluated to determine which one yields the highest vanillin composition by employed CeO_2 nanoparticles as catalyst. The physicochemical properties of the catalyst were characterized using X-ray diffraction, N_2 adsorption-desorption, temperature-programmed oxidation (TPO), and temperature-programmed reduction (TPR) analyses to assess the crystallinity, textural properties, and redox behavior of the CeO_2 nanoparticles. The synthesized CeO_2 nanoparticles showed the presence of diffraction peaks assigned to the presence of cubic fluorite. The N_2 adsorption–desorption isotherms showed that all catalysts possess a Type IV isotherm, indicating a mesoporous structure. From the TPO and TPR profiles, both surface and bulk oxygen species suggest that surface oxygen vacancies play a key role in adsorbing and activating oxygen molecules, leading to a high rate of adsorbed oxygen formation. A direct oxidation method via microwave irradiation with the presence of a nanoparticle catalyst was used to assist the lignin derivation to vanillin production. A test done for all waste samples showed that mesocarp fiber gives the highest vanillin yield of at 6.74% from the direct oxidation method and 11.93% from the lignin extraction method.

Keywords: Direct oxidation; palm oil; vanillin

ABSTRAK

Vanilin mempunyai permintaan pasaran yang tinggi sebagai bahan mentah dalam pelbagai produk harian seperti wangian dan farmaseutikal. Rantaian bekalan vanilin didominasi oleh vanilin sintetik kerana proses penghasilannya lebih digemari serta kos pembuatan yang berkesan. Fokus projek ini adalah untuk memanfaatkan penggunaan biojisim minyak sawit dari Malaysia, sebagai pengeluar utama bahan mentah. Setiap bahagian biojisim minyak sawit seperti pelepah, batang, tandan kosong, tempurung biji dan serat mesokarp, telah dinilai bagi menentukan bahagian yang menghasilkan kandungan vanilin tertinggi. Kaedah pengoksidaan secara langsung melalui pancaran gelombang mikro dengan kehadiran pemangkin cerium(IV) oksida nanozarah telah digunakan untuk membantu penghasilan sintetik vanilin daripada lignin. Keputusan kajian yang dijalankan terhadap semua sampel sisa mendapati bahawa serat mesokarp menghasilkan vanilin tertinggi, iaitu 6.74% melalui kaedah pengoksidaan secara langsung dan 11.93% melalui kaedah pengekstrakan lignin.

Kata kunci: Minyak sawit; pengoksidaan secara langsung; vanilin

INTRODUCTION

In Malaysia, as the world's second-largest producer of crude palm oil, with an annual output exceeding 19 million tons, produces a large amount of lignocellulosic biomass and by-products, the disposal of which is typically costly. Malaysia is the world's second-largest producer of crude palm oil (Chan & Gourich 2024). The country's palm oil industry benefits from diverse biomass components such as mesocarp, EFB, kernel, trunk, and frond, each one rich in valuable content (MIDA 2024). Known for its vigorous growth and high yield, oil palm biomass is highly promising for lignocellulosic valorization. With a balanced syringyl-to-guaiacyl ratio in its lignin content, it has great potential for producing natural vanillin and other value-added products (Romero Pelaez et al. 2024). Vanillin is a flavoring compound that is commonly used in a variety of industries, such as pharmaceuticals, food, drinks, medicine, and perfumery to mask off unwanted smells or aromas (Sikorska 2022). However, a high-quality vanillin bean pod only contains 2% vanillin, which contributes to relatively 1% of global market demand, whereas 88% was dominate by synthetic route, followed by 11.5% from plant-based materials (Walton, Mayer & Narbad 2003). The supply chain is dominated by synthetic vanillin due to its preferred pathway and cost-effective manufacturing. However, the authenticity of natural vanillin retains its unique value as a consumer option (D'Arrigo et al. 2024). This opportunity gap led to the discovery of alternative production methods for natural vanillin from another potential feedstock. One promising route involves the derivation of lignin, due to its aromatic phenolic functional groups that are structurally similar to vanillin.

The monomers that link the molecules of the lignin structure are mostly joined by C-O bonds, which are primarily β-O-4, α-O-4 linkages, as well as C-C bonds. Numerous catalysts have been developed by researchers to specifically cleave the β-O-4 bonds, with metals acting as the main active sites (Jazi et al. 2019; Liu et al. 2024). It has been shown that various catalysts with basicity values can enhance the cleavage of C-O bonds in biomass to a considerable degree (Jian, Meng & Hu 2022). The remarkable redox characteristics of CeO_2 have been clarified by recent research, allowing it to participate in oxidation and reduction events that are essential for converting lignocellulosic components into vanillin (Dong et al. 2025). Wang et al. (2021) reported that CeO_2 promoted the 85% conversion efficiency and 90% selectivity of palm biomass into vanillin. Recent studies done by Liu et al. (2020) have demonstrated the production of 105 mg/g of vanillin. Its large surface area and plenty of surface oxygen vacancies, CeO_2 offers catalytic processes active spots that make reactant molecule binding and activation easier.

Since natural vanillin have a limited production to meet a high market demand, this project focus on the derivation of vanillin from lignin in various palm oil biomass, demonstrating its potential for generating valuable chemical feedstocks (D'Arrigo et al. 2024). There are five different feedstocks which are palm frond, palm trunk, empty fruit bunch, kernel shell, and mesocarp fiber as comparison to identify which precursor can result a high yield of vanillin composition (Chantanumat et al. 2023). The separation process of lignin from cellulose and hemicellulose from lignocellulose of the feedstocks are crucial part to obtain the desired value-added product (Sheraz et al. 2025). According to Wang et al. (2019), extraction of lignin from biomass using conventional method to produce derived vanillin can be conducted with acid, alkaline and enzymes hydrolysis. The acid hydrolysis may remove some amounts of lignin in form of soluble fragments (Carvalho & Colodette 2017), while alkaline hydrolysis pretreatment efficiency is relatively low, and lignocellulose hinder reaction of direct enzyme hydrolysis for the lignin separation (Ying et al. 2018). It was reported that the use of microwave irradiation also able to shorten reaction duration and produced high reaction yields (Qu et al. 2017; Badamali et al. 2013; Oliver 2008) by providing direct heating inside the reaction medium thru efficient hot spots, thereby saving time and energy (Behling, Valange & Chatel 2016). Due to the use of closed reaction vessel, the local heating of reactant molecule was enhanced resulting in accelerated the rate of reaction and the reaction capable to narrow the distribution toward production of selective product. Therefore, method of direct oxidation method with microwave irradiation and CeO_2 nanoparticle catalyst assistance will be conducted for production of vanillin (Anita et al. 2023).

MATERIALS AND METHODS

CATALYST PREPARATION

The CeO_2 nanoparticles were prepared by following the method reported by Anita et al. (2023). First, 0.9 g of $Ce(NO_3)_3.6H_2O$ was added to 60 mL of 5M NaOH solution and stirred for 10 min in a PTFE beaker. Then, the mixture was transferred to a Teflon-lined hydrothermal vessel, sealed and heated to 70 °C for 10 h. After the synthesis duration ended, the hydrothermal was cooled to room temperature before unsealing. The solid was filtered by using vacuum filtration and washed several times with deionized water. The solid was then dried at 120 °C for 16 h and calcination in air at 400 °C 2 h.

CATALYST CHARACTERIZATION

The crystallinity of the CeO_2 catalysts was determined using Bruker X-ray diffraction (XRD) model X'Pert3 Powder and Empyrean (PAN analytical, Billerica, MA, USA). The catalysts were recorded on an X-ray Diffractometer system between 2θ value of 20-80° with 227 s/step exposure time and 0.105 °/step step size. The crystallite size of synthesized CeO_2 nanoparticles were determined according to Scherrer's equation: $D = k\lambda/\beta\cos\theta$. Crystallite size was analyzed using HighScore Plus software (version 3.0), Malvern, UK with X-ray wavelength of CuKα radiation at $\lambda = 1.54$ A, where θ is Bragg angle. β is the full width at half maximum in radians was taken corresponding to the 2θ value at plane (111). The unknown shape factor, k, was assumed as 0.89, the reflecting peak at 2θ was chosen for the entire sample.

Surface area and pore size of the catalysts were analyzed using Brunauer-Emmett-Teller (BET) (Micromeritics ASAP 2020, Norcross, GA, USA). The catalysts were degassed at 200 °C for 24 h, prior to N_2 adsorption measurement at -77 °C. The TPR experiment on H_2 consumption and oxygen capacity storage was conducted on a Thermo Scientific TPDRO 1100 with a

TCD detector. The samples (0.5 g) were treated by heating from 298 to 1073 K at a rate of 10K min^{-1} in a flow of 5 vol% H_2 in He. The total gas flow rate was 10 mL (NTP) min^{-1}. The TPO experiment were conducted on a Thermo Scinetific TPDRO 1100 with a TCD detector. The samples (0.5 g) were treated was treated by heating from 298 to 1073 K at a rate of 10K min^{-1} in a flow of 5 vol% O_2 in He. The total gas flow rate was 10 mL (NTP) min^{-1}.

CATALYST TESTING

The vanillin content of multiple biomass feedstocks, namely empty fruit bunches (EFB), mesocarp fibre, palm kernel, palm frond, and palm trunk were investigated under microwave irradiation with the synthesized CeO_2 nanostructures acting as the reaction catalyst using method by Anita et al. (2023). First, 2 g of grinded and dried biomass was soaked in 20 mL of 0.01 N NaOH solution for 30 min before being transferred to a Teflon tube. After that, 0.3 g of catalyst and 1 mL of H_2O_2 were added to the mixture. The mixture was then heated in a microwave (Milestone, MicroSYNTH MA143) at 170 °C for 20 min. The liquid was then cooled to room temperature and filtered via vacuum filtration and filter paper to eliminate insoluble materials (biomass and catalyst residue). The residue was washed twice with 20 mL solution of 0.01 N NaOH during filtration. The filtrate was then collected into a small beaker. Concentrated hydrochloric acid (37%) was added to the filtrate in a 1:2 ratio and stirred with glass rod for 2 min before being left to cool for 1-2 h. Then, the mixture was centrifuged for 10 min at 2000 rpm using a vortex agitator (Thermo Scientific, Medifuge Centrifuge). The supernatant was then collected and transferred into a separating funnel before it was treated with 1:1 ethyl acetate. After shaking and swirling, the mixture was left to rest before the organic phase was collected and placed into a bottle.

At 60 °C and 289 mbar, excess solvent was evaporated using a rotary evaporator. The slush formed were then dissolved with 1 mL methanol and collected into a vial and sealed. High-Performance Liquid Chromatography (HPLC, Agilent 1200 series HPLC system) with a UV-VIS detector at a wavelength of 280 nm was used to evaluate the brownish solution containing vanillin. A Hypersil C18 column (particle size, 5 m, 150 4.6 mm inner diameter) was used in the HPLC. The column was heated to 35 °C, and a 20 μL injection volume of acetonitrile: water (1:8 v/v) containing 1% acetic acid was used as the mobile phase at a flow rate of 2 mL/min. Vanillin (Sigma-Aldrich, St. Louis, MO, USA, purity 99.7%), syringaldehyde (Sigma-Aldrich, purity 98%), acetosyringone (Sigma-Aldrich, purity 97%), coumaran (Sigma-Aldrich, purity 99%) and syringone (Sigma-Aldrich, purity 99%) were used as standards. A calibration curve for vanillin was constructed so that the amount of vanillin produced could be determined quantitatively.

RESULTS AND DISCUSSION

CATALYST CHARACTERIZATION

The XRD pattern analysis of CeO_2 nanoparticle calcined at 400 °C for 2 h shown in Figure 1. The diffraction peaks at 2thetha (degree) values of 28.53°, 33.07°, 47.46°, 56.31°, 59.06°, 69.38°, 76.66°, and 79.03° correspond to the (111), (200), (220), (311), (222), (400), (331), and (420) planes of the CeO_2 nanoparticles crystal lattice, respectively, that perfectly indexed to ICSD: 81-0792. This observation of CeO_2 peaks comparable with peaks CeO_2 from Jayakumar, Irudayaraj and Raj (2017) and the most prominent peak at (111) plane present the characteristic for the fluorite cubic structure. The peaks are sharp and well-defined, indicating high crystallinity with the mean size of the crystallite nanoparticles CeO_2 equal to 11.3 nm estimated by implementation of the Debye-Scherer equation.

Figure 2 shows the nitrogen adsorption-desorption isotherm of CeO_2 nanoparticles which exhibit Type IV isotherms with type H1 desorption hysteresis based on the International Union of Pure and Applied Chemistry (IUPAC) classification. This indicates the formation of well-developed mesoporous structures (Awoke, Chebude & Díaz 2020). The Type H1 hysteresis loop is typically observed in highly ordered and uniform mesoporous materials, such as MCM-41, MCM-48, and SBA-15 (Thommes et al. 2015).

Table 1 shows the textural properties of CeO_2 nanoparticles catalyst. From the results obtained, the BET surface area for CeO_2 nanoparticles is 66 m^2/g, pore volume is 0.275 cm^3/g and average pore size 27.5 nm, which are relatively high compared to CeO_2 nanorods and nanocubes from our previous works (Anita et al. 2023). In addition, the BET surface area is correlated to the crystallite size of CeO_2 (111) phases obtained from XRD result, as smaller crystallites typically exhibit higher surface areas due to a greater proportion of exposed atoms on the surface. This increased surface exposure enhances the number of active sites available for reactant adsorption and interaction, thereby improving catalytic efficiency (Lykaki et al. 2019). Thus, the synthesized CeO_2 nanoparticles catalyst has sufficient active site to catalyst the extraction of vanillin from palm biomass (Jayakumar, Irudayaraj & Raj 2017).

The catalyst synthesized was further characterized via temperature programmed desorption (TPD). The temperature programmed oxidation of oxygen (O_2-TPO) analysis of the synthesized cerium oxide (IV) catalyst was represented by Figure 3.

The TPO profile exhibits two main O_2 consumption areas with two broad shoulder peaks as highlighted in Figure 3. The first peak around 360 °C is attributed to the oxygen species chemically absorbed by surface oxygen vacancy (O_s) and the peak around 550 °C is attributed to bulk oxygen vacancies (O_b) (Ranga Rao & Mishra 2003). As catalytic reactions only occur on a catalyst's surface,

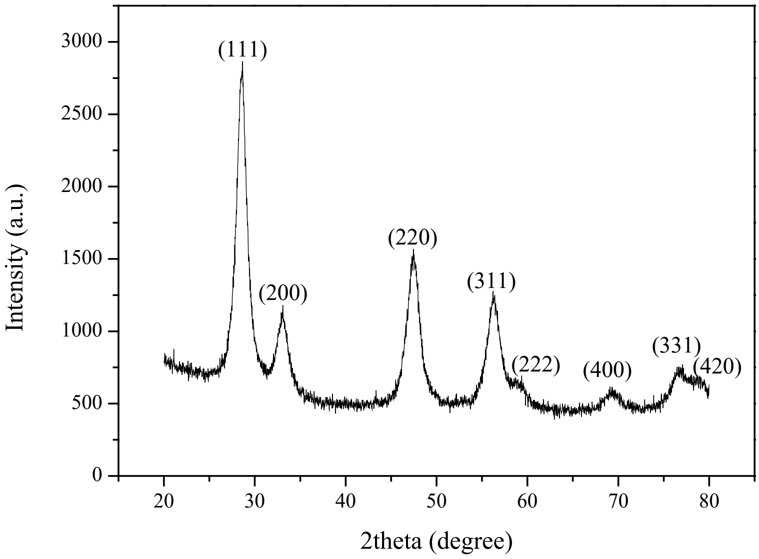

FIGURE 1. XRD pattern of CeO_2 nanoparticles

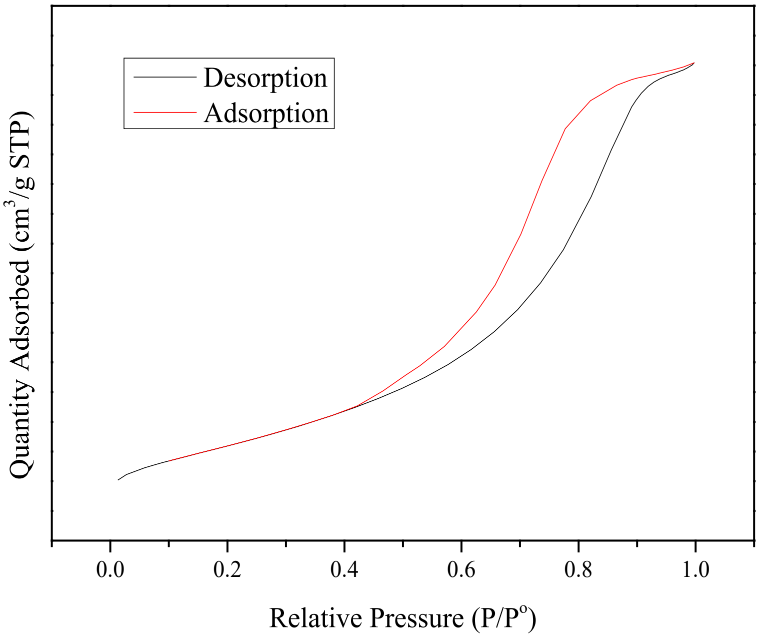

FIGURE 2. N_2 adsorption-desorption of CeO_2 nanoparticles catalyst

TABLE 1. Structural and textural properties of CeO_2 nanoparticles catalyst

Textural properties	Values
BET surface area (m^3/g)	66
Average pore size (nm)	27.5
Pore volume (cm^3/g	0.275
Crystallite size (nm)	11.3

observation of surface/adsorbate interactions is vital to understand the capacity of the CeO_2 to directly oxidize the biomass feedstock to obtain the desired vanillin compound. Based on the high peaks intensity of both surface and bulk oxygen species from the TPO profile, it can be inferred that the surface oxygen vacancy adsorbs and activates oxygen molecules to produce adsorbed oxygen at a high rate and the bulk oxygen peak presence at higher temperature implies a lower electron density and which meant an improved mobility and activity of lattice oxygen species (Tana et al. 2009).

Temperature programmed reduction of hydrogen (H_2-TPR) analysis of CeO_2 is represented by Figure 4. The peak at ~ 450 °C arises from the reduction of Ce^{4+} on the top layers of CeO_2 nanoparticles attributed to the surface oxygen species, whereas the higher peak at ~950 °C arises from the activity of lattice oxygen (bulk oxygen vacancy) (Zhang et al. 2023). Relative to O_2-TPO, the temperature range affected by surface oxygen species and bulk oxygen species provides CeO_2 with excellent redox properties and catalytic oxidation activity (Li et al. 2024).

CATALYST TESTING

High-performance liquid chromatography (HPLC) is a widely used analytical technique in non-volatile liquid samples for quantitative and qualitative analysis. In Figure 5, series of standard vanillin at different concentrations from high to low concentration (1.25×10^{-4}, 6.25×10^{-5}, 3.125×10^{-5}, 1.56×10^{-5} and 7.81×10^{-6}) g/mL was conducted to obtain a standard vanillin calibration curve.

The main purpose of calibration curve is to obtain a linear equation, with R^2 approaching value 1. The formula in Figure 5 used for substitution area under the peak for value y for the gradient allowing to obtain value of concentration vanillin in the product sample. The percentage value for vanillin in respective sample as shown in Tables 2 and 3. The highest yield of vanillin from direct oxidation of biomass is mesocarp with an average of 6.35% followed with frond, EFB, kernel, and trunk. The amount of vanillin influenced the composition of lignin contained in the biomass. The distribution of lignin in lignocellulosic plant influenced by role of lignin in water transport, structural support and natural cell wall barrier, as examples lignin in mesocarps to protect the seeds and support the fruit's weight, and lignin in fronds for the mechanical support and durability (Fache, Boutevin & Caillol 2015). Thus, biomass part with natural abundance lignocellulose theoretically yielding high vanillin (Lourenço & Pereira 2018). Most of the studies primarily focus on empty fruit bunches (EFB), which are the most researched part of the oil palm for vanillin production due to their high lignin content as compared to others palm oil's part. Azizah, Suhartini and Nurika (2021) founds that the biodegradation using rotting fungus *Serpula lacrymans* and ethyl acetate solvent on EFB has yielded approximately 7.3 µg/g of vanillin under optimized conditions of 101.1 mL solvent for 123.5 min of extraction time. On the other hand, studies done by Islam et al. (2025), found that depolymerization of lignin attained approximate 3.9% of vanillin were detected along with 37.62% other lignin-derived product from waste of palm kernel shell by utilizing bimetallic Cu/Co metal on zeolite HY at 180 °C for 2 h using high-pressure reactor. Lignin content of palm kernel shell reported ranging around 45% to 60% (Rezaei, Shafaghat & Daud 2015). In biomass lignin associated with cellulose and hemicellulose in plant cell wall and hindering the accessibility of lignin for the direct oxidation reaction. Kawamoto, Horigoshi and Saka (2007) identified two types of cleavage reactions: The cleavage of the Cβ–O bond and the elimination of the C– group. The former reaction notably results in an increased production of phenolic compounds. Quantum chemistry analyses showed that the Cβ–O bond, with an energy of 90.9 kcal/mol, is more readily broken compared to the Cα–Cβ bond, which has a higher bond energy of 103.8 kcal/mol. In contrast, the O–4 bond (energy: 137.2 kcal/mol) demonstrated the highest stability, followed by the 1–α bond with an energy of 122.5 kcal/mol. Consequently, pyrolysis tends to enhance phenol generation within the polymer structure.

Several studies on production of vanillin from extracted lignin has been explored by using different plant biomass feedstocks as summarized in Table 3. The production yield of vanillin at optimum conditions was used to compare with other biomass feedstocks from literature. The lignin composition was varying with different source of biomass from plant. Our early work on production of vanillin from pineapple leaf lignin yielding 6% with lignin concentration of 6 g/L in 2 M NaOH solution, temperatures 170 °C and pressures 15 bar for 90 min using compressed air as the oxidizing agent and homogeneous sodium hydroxide as catalyst (Kartigaa 2018). The yield of lignin obtained from dried pineapple leaves is 22%. This study was continued by using heterogeneous catalyst of alkaline Ce/MgO on oxidation of kenaf stalk to vanillin which produced 4.3% of vanillin from extracted lignin and 3.8% of vanillin from direct oxidation biomass by using peroxide as oxidizing agent (Anita et al. 2023). Continuous studies were also done by using Ce-based catalyst ($CeZrO_2$–CA) that produced the highest vanillin yield of 9.90% for direct oxidation kenaf stalk for 5 wt% of $CeZrO_2$–CA at 160 °C for 30 min. Furthermore, vanillin production using extracted lignin is studied keeping $CeZrO_2$–CA as a catalyst and with the same operating parameters, which yielded 14.3% of vanillin. Extracted lignin produced from kenaf stalk was 25.7% (Hifza et al. 2023).

Research done by Norzita, Noor Amirah and Mohammad Nasir (2014) obtained a maximum yield of 4.0% vanillin from alkaline oxidation of coconut husk at 160 °C for 2.5 h, using 0.40 mL nitrobenzene as the oxidant. The 25.5% of extracted lignin was produced from Kraft cooking liquor of wood ash reacted with alkaline

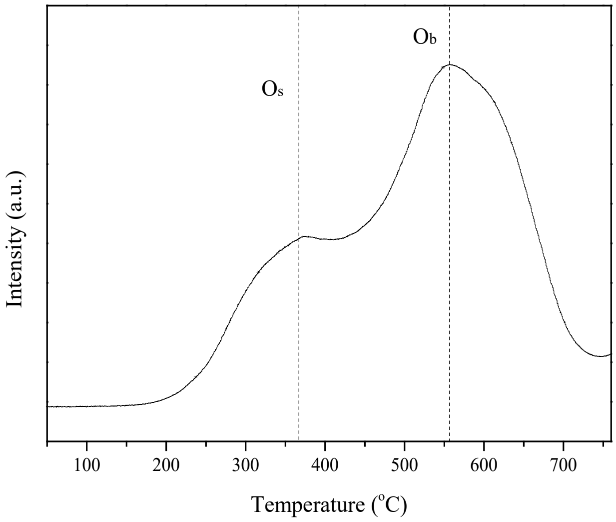

FIGURE 3. Temperature programmed oxidation of oxygen (O_2-TPO) profile

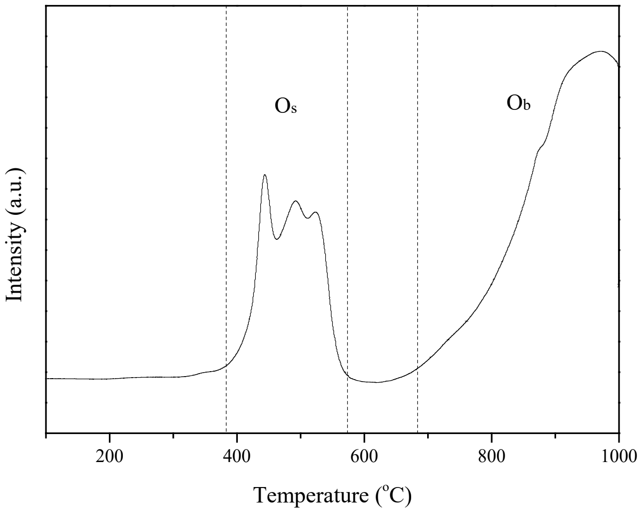

FIGURE 4. Temperature programmed reduction of hydrogen (H_2-TPR) profile

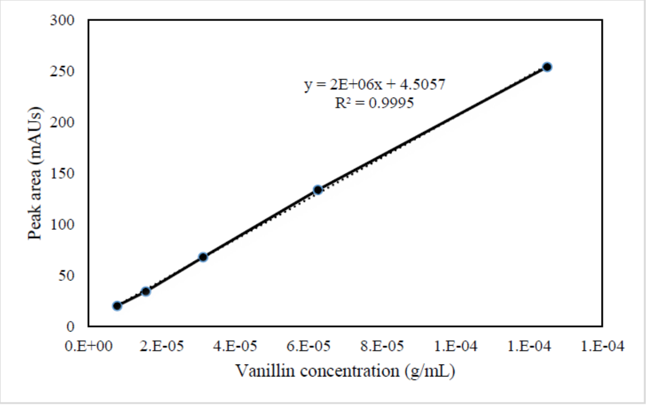

FIGURE 5. Calibration curve of vanillin at 5 different concentrations

TABLE 2. Average percentage yield of vanillin from direct oxidation of palm oil biomass

Sample	Trial	Yield (%)	Average yield (%)
Mesocarp	1	5.94	6.35
	2	6.38	
	3	6.74	
Kernel	1	1.44	1.09
	2	0.94	
	3	0.90	
Empty fruit bunch (EFB)	1	1.88	2.34
	2	2.70	
	3	2.45	
Frond	1	1.92	3.39
	2	3.81	
	3	4.45	
Trunk	1	0.65	0.76
	2	0.91	
	3	0.73	

TABLE 3. Average percentage yield of vanillin from lignin extraction from different plant-biomass reported in literature

Biomass feedstock	Lignin yield (%)	Vanillin yield (%)	Reference
Palm oil mesocarp	24.7	12.2	This work
Kenaf stalk	25.7	14.3	Hifza et al. (2023)
Pineapple leaves	22.0	6.0	Kartigaa (2018)
Coconut husk	39.8	4.0	Norzita, Noor Amirah & Mohammad Nasir (2014)
Wood ash	25.5	3.9	Gitaari et al. (2019)
Rice husk	43	12.0	Zakaria et al. (2023)

nitrobenzene and refluxed at 170 °C for 3 h to obtain vanillin. The vanillin yield obtained from oxidation with nitrobenzene was 3.9% (Gitaari et al. 2019). A Bronsted acidic ionic liquid (BAIL); 1-methyl-3-(3-sulfopropyl)-imidazolium chloride, $[C_3SO_3HMIM]Cl$ was synthesized and commendably used to both assist the depolymerization of lignin from rice husk under mild reaction conditions as well as to benefit from the commercially valuable vanillin. About 68% degree of depolymerization of lignin was achieved under optimized conditions (120 °C, 60 min), yielding 43% of tetrahydrofuran soluble products. The HPLC analysis of the depolymerized lignin detected the clear presence of 12% of vanillin was obtained from 2 wt.% of rice husk's lignin (Zakaria et al. 2023).

Lignin exhibits a heterogeneous structure, predominantly composed of aryl ether linkages, particularly β-O-4 linkages, which account for up to 60% of all structural units. These are followed by β-5, β–β, and other less prominent linkages (Li et al. 2018; Vega-Aguilar, Barreiro & Rodrigues 2021). The strength of lignin's carbon–carbon bonds pose challenges during depolymerization, affecting its reactivity and leading to variations in the resulting products. These variations depend on the depolymerization technique, lignin isolation method, and the source of lignin (Li & Takkellapati 2018; Li et al. 2018; Pérez et al. 2022). Structurally, lignin consists of three main phenylpropanoid units: p-coumaryl alcohol (H-unit), coniferyl alcohol (G-unit), and sinapyl alcohol (S-unit). The composition and arrangement of these units vary across plant species, influencing both the ease of lignin depolymerization and its conversion to vanillin (Araújo, Grande & Rodrigues 2010). For example, lignins with higher β-O-4 linkages are more readily broken down to produce vanillin. Furthermore, lignin composition differs among wood types. Hardwood lignin primarily contains syringyl units derived from sinapyl alcohol, characterized by a greater number of ether bonds due to the presence of two methoxy groups. In contrast, softwood lignin predominantly consists of guaiacyl units derived from coniferyl alcohol (Boerjan, Ralph & Baucher 2003).

The standard of pure vanillin in chromatogram Figure 6(a) as a reference to identify the peak of vanillin in sample product. Figure 6 provides a retention time of a pure vanillin sample at 4.196 min for a first set analysis under the reverse HPLC mode and polar mobile phase and each run analysis a new standard was prepared to reduce error and more precise analysis.

In Figure 6(b), the chromatogram shown for direct mesocarp biomass of vanillin at retention time 4.222 min with another significant peaks at 2.228, 2.763, 3.142, 5.054, 5.206, and 6.830 min. The other compounds could be respectively from phenol, guaiacol, syringone, vanillic acid, syringaldehyde, and acetonesyringone from direct oxidation of mesocarp biomass. The presence of these compounds indicates a complex mixture resulting from the biomass oxidation process, reflecting the multiple pathways of lignin and cellulose degradation.

In comparison, Figure 6(c) shows the chromatogram for the extracted lignin oxidation of mesocarp biomass. The significant difference here is the retention time and the purity of vanillin, with the peak for vanillin observed at 4.613 min. This peak shows higher purity compared to the chromatogram in Figure 6(c). Additionally, the peak for phenol around the retention time of 2.228 min is high and significant in Figure 6(b), indicating a higher concentration of phenol in the direct biomass oxidation compared to the lignin-extracted oxidation.

In contrast, the oxidation of lignin-extracted mesocarp biomass (Figure 6(c)) in the presence of Ce catalysts results in a higher purity and yield of vanillin with 11.93% double the value from direct oxidation biomass. This provides that oxidation of lignin extracted mesocarp in the presence of Ce catalysts increase the purity and yield of vanillin in the product compared with direct oxidation from biomass. Based on the data from previous project obtain highest vanillin yields of 3.70% and 2.90% for extracted lignin and direct biomass oxidation with Ce/MgO catalyst (Nur Akila Syakida Idayu, Anita & Lim 2021). The distinct morphologies of CeO_2 give rise to specific crystal facets that exhibit varying reactivities across different catalytic processes. Theoretically, these active facets on the ceria surface influence the formation of oxygen vacancies and enhance its role as an oxygen donor and acceptor (Hsiao et al. 2007). Our previous findings show that vanillin yields of 4.32% were achieved from extracted lignin from Kenaf stalks, respectively, using the CeO_2 nanoparticles catalyst at 170 °C for 20 min, as compared to CeO_2 nanorods and CeO_2 nanocubes.

Ceria nanoparticles exhibits higher surface chemisorbed oxygen ratio and oxygen storage capacity (OSC) (Anita et al. 2024). The presence of Ce^{3+} ions, alongside oxygen vacancies, significantly enhances the oxidation activity of ceria. This effect is closely linked to the chemisorption of oxygen on the surface, the activation of surface oxygen vacancies, and the migration of oxygen species toward the catalyst surface (Anita et al. 2024; Han, Liu & Gao 2025). Meanwhile, Ce^{4+} acts as an electron acceptor, playing a pivotal role in the rate-limiting step of vanillin synthesis by facilitating the conversion of phenolate anions into phenoxyl radicals. During this process, Ce^{4+} is reduced to Ce^{3+}, which is subsequently reoxidized by hydrogen peroxide (H_2O_2), thereby sustaining oxygen transfer and completing the catalytic redox cycle (Tok et al. 2007; Wu & Heitz 1995). Qualitative analysis of the vanillin extract was carried out using the NIST MS database version 2.2 (2014) library. The composition of compounds detected in the mesocarp extract is listed in Table 4, and the GC chromatogram corresponding to the various identified compounds is shown in Figure 7.

The results reported only major compounds with an area of more than 0.1% detected by GC-MS. The vanillin yield obtained from the extracted lignin from mesocarp was 11.93% using a CeO_2 catalyst at 170 °C for 20 min. In contrast, direct oxidation from the mesocarp yielded an average of 6.35%. Vanillin was successfully extracted from the mesocarp biomass feedstock based on the GC-MS results. Despite the detection of many aromatic and non-aromatic compounds in the products, the amount of vanillin produced is significant. This suggests that vanillin can be produced from mesocarp biomass without the need to separate lignin from the cellulose and hemicellulose components.

Based on Table 4, vanillin was the primary aromatic compound identified from the mesocarp with a very high area. This shows that vanillin is the predominant compound in the extract. Additionally, syringaldehyde, another significant aromatic compound was also detected. Other compounds detected include phenol, guaiacol, coumaran, 4-vinylguaiacol, syringol, acetovanillone, vanillic acid, and acetosyringone. The presence of these chemicals can be explained to the complex nature of the breakdown of lignin throughout the extraction process. Lignin, a heterogeneous polymer consisting of different phenylpropanoid units, undergoes thermal and oxidative breakdown under experimental conditions. Phenol, guaiacol, coumaran, 4-vinylguaiacol, and syringol are all products of lignin breakdown, reflecting the structural diversity within lignin itself (Li & Wilkins 2020). Furthermore, the finding of acetovanillone, vanillic acid, and acetosyringone implies that vanillin and syringaldehyde undergo further oxidative reactions during extraction (Barbosa et al. 2022). Moreover, syringaldehyde has applications that closely mirror those of vanillin due to their nearly identical chemical structures and properties. Both compounds are aromatic aldehydes derived from lignin, with syringaldehyde possessing two methoxy groups compared to vanillin's single methoxy group. However, this structural similarity also makes it challenging to separate syringaldehyde from vanillin due to

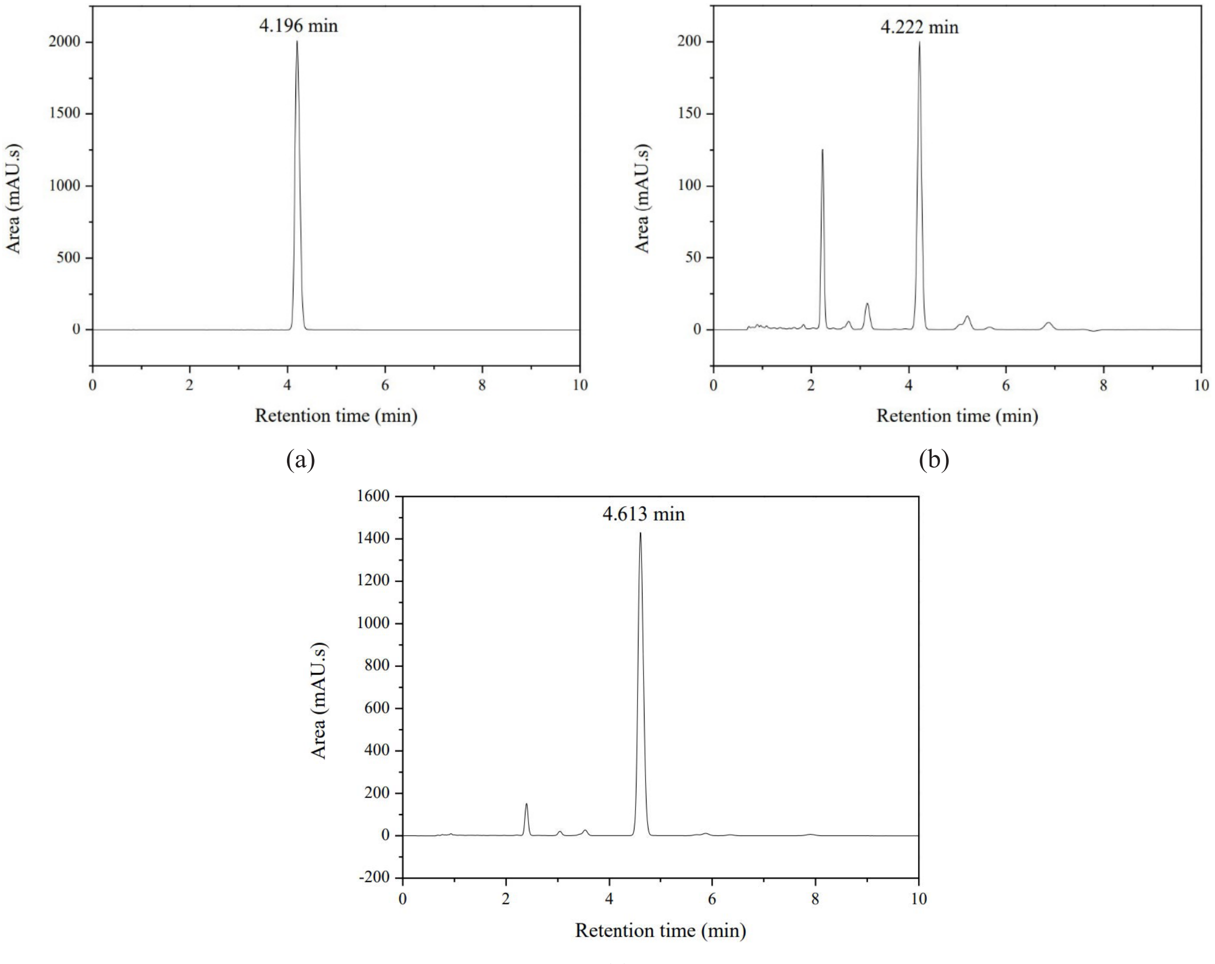

(a) (b)

(c)

FIGURE 6. (a) Chromatogram HPLC of standard vanillin, (b) Chromatogram HPLC vanillin in direct mesocarp biomass, (c) Chromatogram HPLC vanillin of lignin extracted from oil palm mesocarp biomass

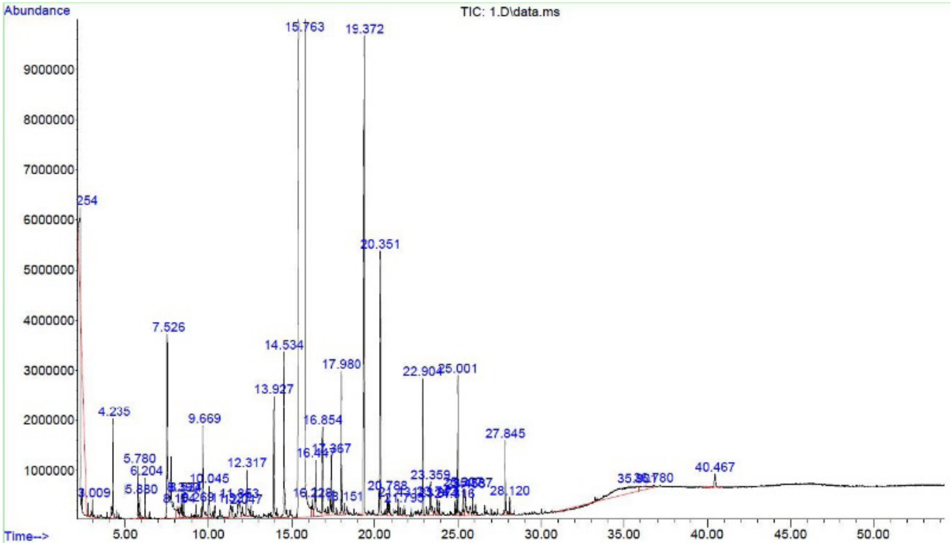

FIGURE 7. GC-MS of detected compounds in the mesocarp

TABLE 4. Details composition of compounds presence in the mesocarp detected by GC-MS

No	Compound	Retention time (min)	Area (%)
1	Phenol	7.67	1.70
2	Guaiacol	9.67	0.57
3	Coumaran	12.31	0.38
4	4-vinylguaiacol	13.93	0.75
5	Syringol	14.53	1.23
6	Vanillin	15.80	48.33
7	Acetovanillone	16.85	0.52
8	Vanillin acid	17.30	0.12
9	Syringaldehyde	19.38	4.26
10	Acetosyringone	20.36	1.68

their comparable boiling points, solubility, and behavior in chromatographic separation methods (Rodrigues, Borges & Rodrigues 2012).

CONCLUSION

In this study, CeO_2 nanoparticles were successfully synthesized and characterized as an effective catalyst for the direct oxidation of various oil palm biomass components, including mesocarp, empty fruit bunches (EFB), kernel, trunk, and frond. The approach bypassed the conventional separation of cellulose and hemicellulose from the lignocellulosic matrix, offering a greener and more time-efficient process. Among the tested feedstock, mesocarp biomass yielded the highest vanillin output at 6.35%. Notably, extraction of lignin from the mesocarp further enhanced the yield to 12.20% under 170 °C for 20 min using microwave irradiation at 300 W, with 15 wt.% CeO_2 nanoparticles catalyst and H_2O_2 as the oxidant. The catalytic performance was attributed to the redox cycling between Ce^{4+} and Ce^{3+}, facilitated by CeO_2's high oxygen storage capacity. The regeneration of Ce^{4+} via H_2O_2 maintained the redox cycle and promoted efficient oxygen transfer, thereby improving both reaction efficiency and selectivity toward vanillin.

ACKNOWLEDGEMENTS

We would like to thank the Ministry of Higher Education, Malaysia under the Fundamental Research Grant Scheme (FRGS/1/2020/STG04/UTP/02/2, cost centre 015MA0-125, funder ID 10.13039/501100003093) for the research grants awarded to conduct the research. We are deeply grateful to FELCRA Nasaruddin, Perak for providing the biomass waste materials essential for this research as well as for their assistance and guidance throughout the collection of the sample for this study.

REFERENCES

Anita Ramli, Nur Akila Syakida Idayu Khairul Anuar, Normawati Mohamad Yunus & Alina Rahayu Mohamed. 2024. Synthesis of vanillin via oxidation of kenaf stalks in the presence of CeO_2: Tuning the catalytic behaviour of CeO_2 via nanostructure morphology. *RSC Advances* 14(49): 36327-36339.

Anita Ramli, Nur Akila Syakida Idayu Khairul Anuar, Nur Aielia Amira Bakhtiar, Normawati Mohamad Yunus & Alina Rahayu Mohamed. 2023. Direct oxidation of *Hibiscus cannabinus* stalks to vanillin using CeO_2 nanostructure catalysts. *Molecules* 28(13): 4963.

Araújo, J.D., Grande, C.A. & Rodrigues, A.E. 2010. Vanillin production from lignin oxidation in a batch reactor. *Chemical Engineering Research and Design* 88(8): 1024-1032.

Awoke, Y., Chebude, Y. & Díaz, I. 2020. Controlling particle morphology and pore size in the synthesis of ordered mesoporous materials. *Molecules* 25(21): 4909.

Azizah, N., Suhartini, S. & Nurika, I. 2021. Optimization of vanillin extraction from biodegradation of oil palm empty fruit bunches by *Serpula lacrymans*. *Industria Jurnal Teknologi dan Manajemen Agroindustri* 10(1): 33-40.

Badamali, S.K., Luque, R., Clark, J.H. & Breeden, S.W. 2013. Unprecedented oxidative properties of mesoporous silica materials: Towards microwave-assisted oxidation of lignin model compounds. *Catalysis Communications* 31: 1-4.

Barbosa, B.M., Vaz Jr., S., Colodette, J.L., de Aguiar, A.R., Távora Cabral, C.P. & de Freitas Homem de, B. 2022. Structural and chemical characterization of lignin and hemicellulose isolated from corn fibers toward agroindustrial residue valorization. *Cellulose* 29(15): 8117-8132.

Behling, R., Valange, S. & Chatel, G. 2016. Heterogeneous catalytic oxidation for lignin valorization into valuable chemicals: What results? What limitations? What trends? *Green Chemistry* 18(7): 1839-1854.

Boerjan, W., Ralph, J. & Baucher, M. 2003. Lignin biosynthesis. *Annual Review of Plant Biology* 54(1): 519-546.

Carvalho, D.M. & Colodette, J.L. 2017. Comparative study of acid hydrolysis of lignin and polysaccharides in biomasses. *BioResources* 12(4): 6907-6923.

Chan, E.S. & Gourich, W. 2024. Palm oil: From environmental villain to climate hero. *Malay Mail*, August 16.

Chantanumat, Y., Phetwarotai, W., Sangthong, S., Palamanit, A., Abu Bakar, M.S., Cheirsilp, B. & Phusunti, N. 2023. Characterization of bio-oil and biochar from slow pyrolysis of oil palm plantation and palm oil mill wastes. *Biomass Conversion and Biorefinery* 13: 13813-13825.

D'Arrigo, P., Rossato, L.A.M., Strini, A. & Serra, S. 2024. From waste to value: Recent insights into producing vanillin from lignin. *Molecules* 29(2): 442.

Dong, Y.G., Kong, W.J., Ma, Z., Yang, Y., Wang, P., Sheng, S.X., Dong, L., Gu, X.L. & Chen, Z.P. 2025. Insight into the morphology-dependent CeO_2 for oxidation of lignin model compounds via C–C bond cleavage. *Rare Metals* 44: 4767-4778.

Fache, M., Boutevin, B. & Caillol, S. 2015. Vanillin production from lignin and its use as a renewable chemical. *ACS Sustainable Chemistry & Engineering* 4(1): 35-46.

Gitaari, N., Benard, K., Gichuki, J. & Kareru, P. 2019. Synthesis of vanillin from lignin. *Chemical Science International Journal* 27(1): 1-5.

Han, Z., Liu, W. & Gao, Y. 2025. Advancing the understanding of oxygen vacancies in ceria: Insights into their formation, behavior, and catalytic roles. *JACS Au* 5: 1549-1569.

Hifza Rouf, Anita Ramli, Nur Akila Syakida Idayu Khairul Anuar & Normawati Mohamad Yunus. 2023. Ce–Zr-based mixed oxide catalyst for oxidative depolymerization of kenaf stalk (biomass) into vanillin. *Bioresources and Bioprocessing* 10: 76.

Hsiao, W., Lin, Y., Chen, Y. & Lee, C. 2007. The effect of the morphology of nanocrystalline CeO_2 on ethanol reforming. *Chemical Physics Letters* 441(4-6): 294-299.

Islam, M.K., Kongparakul, S., Guan, G., Chanlek, N. & Samart, C. 2025. Oxidative fractionation of palm kernel shell waste biomass over bimetallic Co-Cu/Zeolite HY catalyst. *Biomass and Bioenergy* 193: 107609.

Jayakumar, G., Irudayaraj, A.A. & Raj, A.D. 2017. Particle size effect on the properties of cerium oxide (CeO_2) nanoparticles synthesized by hydrothermal method. *Mechanics, Materials Science & Engineering Journal* 9: doi:10.2412/mmse.3.4.481

Jazi, M.E., Narayanan, G., Aghabozorgi, F., Farajidizaji, B., Aghaei, A., Kamyabi, M.A., Navarathna, C.M. & Mlsna, T.E. 2019. Structure, chemistry, and physicochemistry of lignin for material functionalization. *SN Applied Sciences* 1: 1094.

Jian, Y., Meng, Y. & Hu, L. 2022. Selectivity control of C-O bond cleavage for catalytic biomass valorization. *Frontiers in Energy Research* 9: 827680.

Kartigaa, H. 2018. Synthesis of renewable vanillin from pineapple leaves lignin. FYP Dissertation. Universiti Teknologi PETRONAS (Unpublished).

Kawamoto, H., Horigoshi, S. & Saka, S. 2007. Pyrolysis reactions of various lignin model dimers. *Journal of Wood Science* 53(2): 168-174.

Li, M. & Wilkins, M. 2020. Lignin bioconversion into valuable products: Fractionation, depolymerization, aromatic compound conversion, and bioproduct formation. *Systems Microbiology and Biomanufacturing* 1(2): 166–185.

Li, J., Zhou, S., Wan, Q., Guo, H. & Lin, S. 2024. Elucidating the intrinsic relationship between redox properties of CeO_2 and CH_4 oxidation activity: A theoretical perspective. *The Journal of Chemical Physics* 161(17): 174707.

Li, T. & Takkellapati, S. 2018. The current and emerging sources of technical lignins and their applications. *Biofuels Bioproducts and Biorefining* 12(5): 756-787.

Li, Y., Shuai, L., Kim, H., Motagamwala, A.H., Mobley, J.K., Yue, F., Tobimatsu, Y., Havkin-Frenkel, D., Chen, F., Dixon, R.A., Luterbacher, J.S., Dumesic, J.A. & Ralph, J. 2018. An "ideal lignin" facilitates full biomass utilization. *Science Advances* 4(9). https://doi.org/10.1126/sciadv.aau2968

Liu, Q., Yang, D., Zhao, X., Xu, Z., Ding, J., Wu, D., An, N., Liao, H. & Hou, Z. 2024. Oxidative cleavage of β-O-4 bonds in lignin model compounds with polymer-supported Ni–Salen catalysts. *RSC Sustainability* 2: 3397-3408.

Lourenço, A. & Pereira, H. 2018. Compositional variability of lignin in biomass. In *Lignin - Trends and Applications*. pp. 65-98. http://dx.doi.org/10.5772/intechopen.71208

Lykaki, M., Stefa, S., Carabineiro, S., Pandis, P., Stathopoulos, V. & Konsolakis, M. 2019. Facet-dependent reactivity of Fe_2O_3/CeO_2 nanocomposites: Effect of ceria morphology on CO oxidation. *Catalysts* 9(4): 371.

Malaysian Investment Development Authority (MIDA). 2024. Diverse biomass components in Malaysia's palm oil industry. Food technology - Palm biomass.

Norzita Ngadi, Noor Amirah Abdul Halim & Mohammad Nasir Mohamad Ibrahim. 2014. Isolation and characterization of vanillin from coconut husk lignin via alkaline nitrobenzene oxidation. *Jurnal Teknologi* 67(4): 19-23.

Nur Akila Syakida Idayu Khairul Anuar, Anita Ramli & Lim Jun Wei. 2021. Synthesis of Ce/MgO catalysts for direct oxidation of *Hibiscus cannabinus* stalks to vanillin. *Catalysts* 11(12): 1449.

Pérez, E., Abad-Fernández, N., Lourençon, T., Balakshin, M., Sixta, H. & Cocero, M.J. 2022. Base-catalysed depolymerization of lignins in supercritical water: Influence of lignin nature and valorisation of pulping and biorefinery by-products. *Biomass and Bioenergy* 163: 106536.

Qu, C., Kaneko, M., Kashimura, K., Tanaka, K., Ozawa, S. & Watanabe, T. 2017. Direct production of vanillin from wood particles by copper oxide–peroxide reaction promoted by electric and magnetic fields of microwaves. *ACS Sustainable Chemistry & Engineering* 5(12): 11551-11557.

Ranga Rao, G. & Mishra, B.G. 2003. Structural, redox, and catalytic chemistry of ceria-based materials. *Bulletin of Catalysis Society of India* 2: 122-134.

Rezaei, P.S., Shafaghat, H. & Wan Daud, W.M.A. 2015. Aromatic hydrocarbon production by catalytic pyrolysis of palm kernel shell waste using a bifunctional Fe/H-Beta catalyst: Effect of lignin-derived phenolics on zeolite deactivation. *Green Chemistry* 18(6): 1684-1693.

Rodrigues Pinto, P.C., Borges da Silva, E.A. & Rodrigues, A.E. 2012. Lignin as source of fine chemicals: Vanillin and syringaldehyde. In *Biomass Conversion*, edited by Baskar, C., Baskar, S. & Dhillon, R. Springer, Berlin, Heidelberg. pp. 381-420.

Romero Pelaez, R.D., Oliveira, M.E.C., Miller, R.N.G., Almeida, J.R.M. & de Siqueira, F.G. 2024. Biotechnological valorization of lignocellulosic residues from the oil palm industry: Status and perspectives. *Biomass Conversion and Biorefinery* 14: 3077-3099.

Sheraz, M., Cao, L., Zhao, S., Gao, H., Dansawad, P., Xue, C., Li, Y. & Li, W. 2025. Lignocellulosic biomass pretreatment methods and application of extracted fractions. *Arabian Journal for Science and Engineering* 50: 3717-336.

Sikorska, J. 2022. Vanillin and its applications in the food and pharmaceutical industries. *Foodcom S.A.* https://foodcom.pl/en/vanillin-and-its-applications-in-the-food-and-pharmaceutical-industries/

Tana, Zhang, M., Li, J., Li, H., Li, Y. & Shen, W. 2009. Morphology-dependent redox and catalytic properties of CeO_2 nanostructures: Nanowires, nanorods, and nanoparticles. *Catalysis Today* 148: 179-183.

Thommes, M., Kaneko, K., Neimark, A.V., Olivier, J.P., Rodriguez-Reinoso, F., Rouquerol, J. & Sing, K.S.W. 2015. Physisorption of gases, with special reference to the evaluation of surface area and pore size distribution (IUPAC Technical Report). *Pure and Applied Chemistry* 87(9-10): 1051-1069.

Tok, A., Du, S., Boey, F. & Chong, W. 2007. Hydrothermal synthesis and characterization of rare earth doped ceria nanoparticles. *Materials Science and Engineering A* 466(1-2): 223-229.

Walton, N.J., Mayer, M.J. & Narbad, A. 2003. Vanillin. *Phytochemistry* 63(5): 505-515.

Wang, H., Zou, Y., Sun, H., Chen, Y., Li, S. & Lan, Y. 2021. Recent progress and perspectives in heterogeneous photocatalytic CO_2 reduction through a solid-gas mode. *Coordination Chemistry Reviews* 438: 213906.

Wang, H., Pu, Y., Ragauskas, A. & Yang, B. 2019. From lignin to valuable products-strategies, challenges, and prospects. *Bioresource Technology* 271: 449-461.

Wu, G. & Heitz, M. 1995. Catalytic mechanism of Cu^{2+} and Fe^{3+} in alkaline O_2 oxidation of lignin. *Journal of Wood Chemistry and Technology* 15(2): 189-202.

Vega-Aguilar, C.A., Barreiro, M.F. & Rodrigues, A.E. 2021. Lignin conversion into C4 dicarboxylic acids by catalytic wet peroxide oxidation using titanium silicalite-1. *Industrial Crops and Products* 173: 114155.

Ying, W., Shi, Z., Yang, H., Xu, G., Zheng, Z. & Yang, J. 2018. Effect of alkaline lignin modification on cellulase–Lignin interactions and enzymatic saccharification yield. *Biotechnology for Biofuels* 11: 214.

Zakaria, S.M., Idris, A., Chandrasekaram, K., Darji, D. & Alias, Y. 2023. Rice husk lignin to vanillin: IonoSolv as a way forward for value-added biomass depolymerization. *BioResources* 18(3): 5385-5398.

Zhang, G., Zhou, Y., Yang, Y., Kong, T., Song, Y., Zhang, S. & Zheng, H. 2023. Elucidating the role of surface Ce^{4+} and oxygen vacancies of CeO_2 in catalytic activity. *Molecules* 28(9): 3785.

*Corresponding author; email: anita_ramli@utp.edu.my